AAM for Wang L. et al., UCMMT, September 2017, Liverpool, UK.

Design of a Ka-band MW-level High Efficiency Gyroklystron for Accelerators

Li Wang, Kun Dong, Jianxun Wang, Yong Luo
School of Physical Electronics
University of Electronic Science and Technology of China
Chengdu, China, 610054
wli2012@uestc.edu.cn

Wenlong He, Adrian W. Cross, Kevin Ronald, Alan D. R. Phelps
Department of Physics, SUPA
University of Strathclyde
Glasgow, Scotland, UK, G4 0NG
w.he@strath.ac.uk

***Abstract*—Design of a three-cavity Ka-band MW-level gyroklystron operated at the fundamental TE_{02} mode is presented in this paper. The initial design of the magnetron injection gun (MIG) and interaction circuit has been completed by using the PIC (Particle in cell) code MAGIC. The PIC simulation shows this gyroklystron can deliver an output power of more than 1.5 MW with a gain of > 35 dB at 36 GHz. The achieved efficiency exceeds 40 % when driven by a 95 kV, 45 A beam. The optimized MIG has a transverse velocity spread of less than 2.5% when the velocity ratio is around 1.3.**

Keywords—gyroklystron; Ka-band; MIG; interaction circuit

I. Introduction

Gyroklystrons are vacuum electronic devices (VEDs) which can produce high power in the millimeter and submillimeter wave bands [1-2]. The applications of gyroklystrons include radar systems, remote communication, material processing, etc [3-4]. As a millimeter wave high power source for accelerator, a Ka-band gyroklystron is being studied at the University of Strathclyde and UESTC. The initial design has been completed. A stable output power of more than 1.5 MW is predicted with an efficiency of more than 40%.

II. MIG Design

This Ka-band gyroklystron is driven by a triode type MIG which can generate small-orbit electrons [6]. Compared with the diode type MIG, the triode type version has a better control on the beam parameters, especially the beam velocity ratio (v_t/v_z, where v_t and v_z are transverse and axial velocity components, respectively.) [7]. By adjusting the modulating anode voltage, the velocity ratio of the electron beam can be fine-tuned without incurring obvious deterioration of the velocity spread. The configuration of this Ka-band triode type MIG is shown in Fig. 1. The electron trajectories are denoted in red lines. A circle of dielectric material is mounted inside the waveguide wall at the gun exit to avoid exciting parasitic modes.

The simulation results show that all electrons have passed the gun tunnel without any interception. The optimized beam transverse and axial velocity spreads are less than 5% when the the velocity ratio is maintained around 1.3. The average beam guiding center radius is 2.25 mm. The beam current and voltage are 45 A and 95 kV, respectively. The optimized parameters of the gun are summarized in TABLE I.

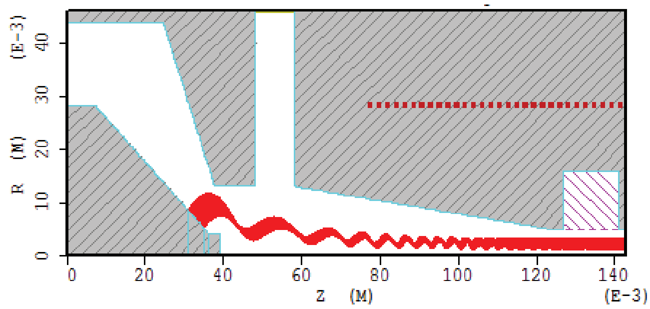

Fig. 1. Beam trajectories and gun configuration of Ka-band MIG.

TABLE I MIG Parameters

Parameters	Value
Cathode angle φ_c (deg)	39.7
Emitter width L_s (mm)	5.23
Emitter average radius R_c (mm)	6.85
Current I_0 (A)	45
Anode voltage V_0 (kV)	95
Modulating anode voltage V_m (kV)	38.5
Magnetic field @ gun exit B_0 (T)	1.34
Magnetic compression ratio f_m	10.5
Velocity ratio α	1.31
Transverse velocity spread $\Delta\beta_t$ (%)	2.31
Axial velocity spread $\Delta\beta_z$ (%)	4.09
Mean guiding center radius r_{g0} (mm)	2.25

Fig. 2 shows the dependence of velocity ratio α and transverse velocity spread $\Delta\beta_t$ as functions of modulating anode voltage V_m. As V_m grows from 37.5 kV to 38.9 kV, α almost linearly increases from 1.1 to 1.4 due to the transverse acceleration of the modulating anode, while $\Delta\beta_t$ slightly varies around 2.5%. The results of sensitivity studies show that the MIG can be operated stably within reasonable parametric windows, which demonstrates a robust MIG design.

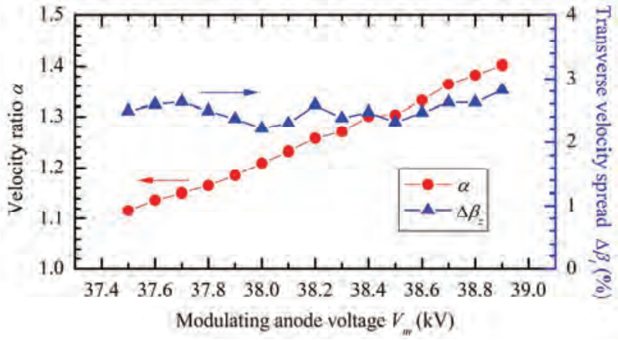

Fig. 2. Velocity ratio and transverse velocity spread as functions of modelating anode voltage.

III. Interaction Circuit Design

According to application requirements of University of Strathclyde, The Ka-band gyroklystron employs a three-cavity configuration. A dielectric material has been applied to overcome mode competition problems. The electron beam is tuned by the injected microwave in the first cavity and the bunching is strengthened in the second cavity. Finally in the third cavity, most electrons lose their energy and the microwave radiation is amplified. Fig. 3 shows the configuration of the interaction structure as well as the bunching process of the electron beams. A distinct change of electron status is observed in the output cavity, where the efficient beam-wave interaction occurs. In the collector zone, under the force of declining magnetic field, the electron beams and amplified microwave are well separated and the residual electrons are collected by the inner walls.

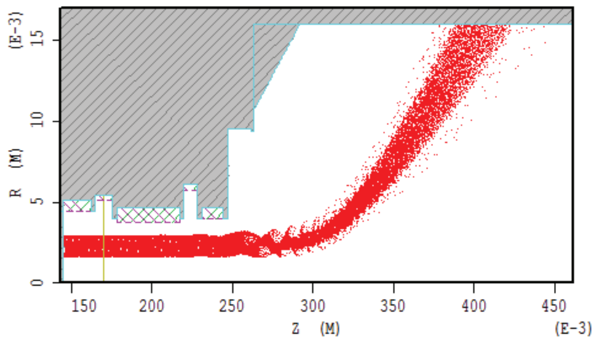

Fig. 3. Plot of electron trajectories showing the bunching process.

The evolution of the relativistic factor gamma of electron beam as a function of axial distance is given in Fig. 4. It is shown that when entering the output cavity, most of the electrons begin to lost their energy and the electrons are well bunched with the input signal amplified effectively.

The evolution of output power with regard to the simulating time is given in Fig. 5. After 10 ns, the output power is stabilized at 1.9 MW. A pure TE_{02} mode has been amplified in the output cavity. The Fourier transformation of angular electric field at the output port shows there is a distinct frequency component of 36 GHz existing in the frequency spectrum. No other frequency components are found except a relatively weak 2rd harmonic frequency component of 72 GHz.

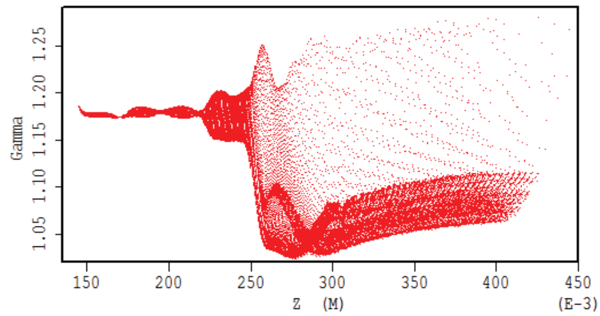

Fig. 4. Relativistic factor versus axial distance.

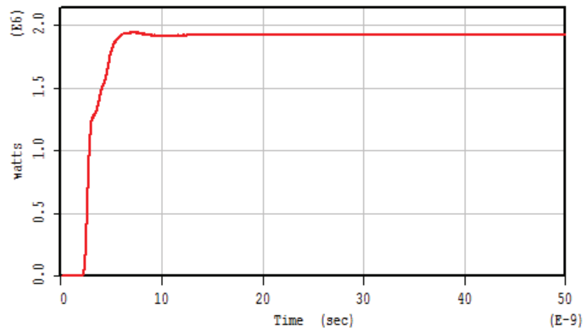

Fig. 5. Ouput power as a function of the time.

The dependence of output power as a function of the frequency is shown in Fig. 6. The maximum output power is achieved at 36 GHz. The estimated 3 dB bandwidth is about 700 MHz, note that in the PIC simulation, zero beam velocity spread is considered. So in the actural operation of the gyroklystron, both the maximum output power and the 3 dB bandwidth will be decreased.

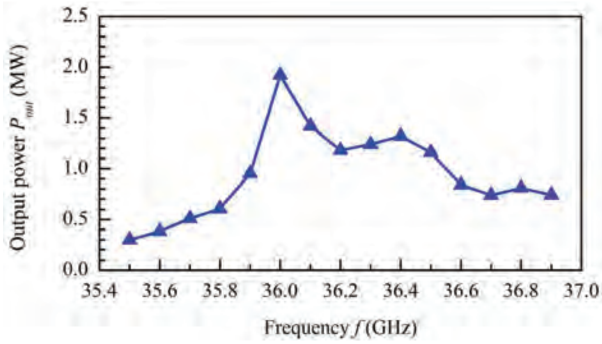

Fig. 6. Output power versus frequency.

IV. Conclusion

A design of a Ka-band gyroklystron has been accomplished by using PIC simulations. Fabrication and test of the cavities will be completed in the near future.

References

[1] M. Blank, Bruce G. Danly, Baruch Levush, and D. E. Pershing, “Experimental investigation of W-band (93 GHz) gyroklystron amplifiers,” IEEE Trans. Plasma Sci., vol. 26, pp. 409–415, June 1998.

[2] J. J. Choi, A. H. McCurdy, F. N. Wood, R. H. Kyser, J. P. Calame, K. T. Nguyen, B. G. Danly, T. M. Antonsen, B. Levush, and R. K. Parker, “Experimental investigation of a high power, two-cavity, 35 GHz gyroklystron amplifier,” IEEE Trans. Plasma Sci., Vol. 26, no. 3, pp. 416–425, Jun. 1998.

[3] Granatstein and W. Lawson, “Gyro-amplifiers as candidate RF-drivers for TeV linear colliders,” IEEE Trans. Plasma Sci., vol. 24, p. 648, June 1996.

[4] M. Thumm, State-of-the-Art of High Power gyro-Devices and Free Electron Maser. Karlsruhe, Germany: KIT Publishing, 2012.

[5] B. Goplen, L. Ludeking, D. Smith, and G. Warren, “User-configurable MAGIC for electromagnetic PIC calculations,” Comput. Phys. Commun., vol. 87, nos. 1–2, pp. 54–86, May 1995.

[6] J. M. Baird and W. Lawson, “Magnetron injection gun (MIG) design for gyrotron applications,” Int. J. Electron., vol. 61, no. 6, pp. 953–967, Dec. 1986.

[7] W. Lawson and V. Specht, “Design comparison of single-anode and double-anode 300-MW magnetron injection gun,” IEEE Trans. Electron Devices, vol. 40, no. 7, pp. 1322–1328, Jul. 1993.

[8] J. P. Calame, M. Garven, J. J. Choi, K. Nguyen, F. Wood, M. Blank, B. G. Danly, and B. Levush, “Experimental studies of bandwidth and power production in a three-cavity 35 GHz gyroklystron amplifier,” Phys. Plasmas, vol. 6, no. 1, pp. 285–297, Jan. 1999.